Conference Paper, Published Version

Gotoh, Hitoshi; Khayyer, Abbas

Improved MPS Methods for Refined Simulation of Free-Surface Hydrodynamic Flows

IMPROVED MPS METHODS FOR REFINED SIMULATION OF FREE-SURFACE HYDRODYNAMIC FLOWS

Hitoshi Gotoh[1] and Abbas Khayyer[2]

[1] Professor, Department of Urban and Environmental Engineering, Kyoto University
Katsura Campus, Nishikyo-ku, Kyoto, 615-8540, Japan, e-mail: gotoh@mbox.kudpc.kyoto-u.ac.jp
[2] Doctoral student, Department of Urban and Environmental Engineering, Kyoto University
Katsura Campus, Nishikyo-ku, Kyoto, 615-8540, Japan, e-mail: khayyer@wfee.mbox.media.kyoto-u.ac.jp

ABSTRACT

As a gridless particle method, the MPS (Moving Particle Semi-implicit) method has been proven useful in a wide variety of engineering applications including free-surface hydrodynamic flows. Despite its simplicity and wide range of applicability, the MPS method suffers from some drawbacks such as non-conservation of momentum and spurious pressure fluctuation. By introducing new formulations for pressure gradient and source term of Poisson Pressure Equation (PPE), we have proposed improved MPS methods for refined simulation of free-surface hydrodynamic flows. The enhanced performance of the proposed methods is shown through the simulation of numerous free-surface hydrodynamic flows in comparison with the experimental data.

Keywords: particle method, MPS method, momentum conservation, pressure fluctuation

1. INTRODUCTION

Free-surface hydrodynamic flows are of significant industrial and environmental importance, yet, are difficult to simulate due to the presence of an arbitrary moving interface. A recent interest has been focused on the development of Lagrangian gridless methods, namely the particle methods. Due to their inherent gridless feature, particle methods are well suited for treatment of problems characterized by moving discontinuities and large deformations. In addition, because of their Lagrangian nature, such methods can analyze problems without the numerical diffusion arising from fixed-point interpolations of advective terms as in case of Eulerian grid-based methods. Accordingly, particle methods provide a substantial potential for simulation of free-surface hydrodynamic flows, especially those accompanied by large deformations and fragmentations. Particle methods can be classified into those based on field approximations, as the Element-Free Galerkin method (EFG), and those based on kernel approximations, as the Smoothed Particle Hydrodynamics (SPH) or Moving Particle Semi-implicit (MPS) methods.

Originally developed by Koshizuka and Oka (1996), the MPS method has been proven useful in a wide variety of engineering applications including free-surface hydrodynamic flows (e.g. Gotoh and Sakai, 1999; Gotoh et al., 2005). Despite its wide range of applicability, the MPS method suffers from some inherent difficulties such as non-conservation of momentum (Khayyer and Gotoh, 2008) and spurious pressure fluctuation (Gotoh et al., 2005).

By focusing on the momentum conservation properties of original MPS formulations, we have proposed a new pressure gradient term which conserves both linear and angular momentum. The MPS method modified by the new pressure gradient term has been given the name CMPS (Corrected MPS). The enhanced performance of CMPS method is shown through the simulation of a plunging breaker and resultant splash-up. Further refined reproduction of the splash-up is obtained by applying a tensor-type strain-based viscosity by CMPS-SBV (CMPS with a Strain-Based Viscosity) method.

To resolve the problem of spurious pressure fluctuation, derivation of the Poisson Pressure Equation (PPE) in MPS method is revisited. It is shown that the original PPE in MPS method has been derived on the basis of an assumption which is not fully valid as a result of the existence of numerical errors due to particle-based discretization. Accordingly, calculation of pressure in original (standard) MPS method comes with considerable pressure fluctuations which do not allow the method to be applied as a reliable numerical tool for the prediction of, for instance, wave impact pressure on a coastal structure. To obtain a less-fluctuating and more-accurate pressure field, a higher order source term of PPE is derived. The CMPS method modified by the new source term has been given the name CMPS-HS (CMPS with a Higher-order Source term). The improved performance of CMPS-HS method, as well as its applicability for calculation of wave impact pressure, are shown through the simulation of a dam break with impact (Hu and Kashiwagi, 2004) and a flip-through impact (Hattori et al., 1994).

2. MPS METHOD; BRIEF DESCRIPTION

Here the MPS method is briefly explained. Detailed descriptions were provided by Koshizuka and Oka (1996) or Gotoh et al. (2005). The governing equations are the continuity and Navier-Stokes equations describing the motion of a viscous incompressible flow:

$$\nabla \cdot \boldsymbol{u} = 0 \tag{1}$$

$$\frac{\mathrm{D}\boldsymbol{u}}{\mathrm{D}t} = -\frac{1}{\rho}\nabla p + \boldsymbol{g} + \nu \nabla^2 \boldsymbol{u} \tag{2}$$

where $\boldsymbol{u}$ = particle velocity vector; t = time; ρ = fluid density; p = particle pressure; $\boldsymbol{g}$ = gravitational acceleration vector and ν = laminar kinematic viscosity.

The gradient operator is defined as a local weighted average of the gradient vectors between particle i and its neighboring particles j:

$$\langle \nabla \phi \rangle_i = \frac{D_s}{n_0} \sum_{j \neq i} \frac{\phi_j - \phi_i}{\left|\boldsymbol{r}_j - \boldsymbol{r}_i\right|^2} (\boldsymbol{r}_j - \boldsymbol{r}_i)\, w\left(\left|\boldsymbol{r}_j - \boldsymbol{r}_i\right|\right) \tag{3}$$

where ϕ = arbitrary scalar function, D_s = number of space dimensions, $\boldsymbol{r}$ = coordinate vector of fluid particle, $w(r)$ = the kernel function and n_0 = the constant particle number density. Following Koshizuka et al. (1998), the pressure gradient is defined by replacing ϕ_i in Eq. 3 by the minimum value of ϕ among the neighboring particles, such as:

$$\langle \nabla p \rangle_i = \frac{D_s}{n_0} \sum_{j \neq i} \frac{p_j - \hat{p}_i}{\left|\boldsymbol{r}_j - \boldsymbol{r}_i\right|^2} (\boldsymbol{r}_j - \boldsymbol{r}_i)\, w\left(\left|\boldsymbol{r}_j - \boldsymbol{r}_i\right|\right) \tag{4}$$

$$\hat{p}_i = \min_{j \in J} (p_i, p_j) \quad , \; J = \left\{ j : w\left(\left|\boldsymbol{r}_j - \boldsymbol{r}_i\right|\right) \neq 0 \right\} \tag{5}$$

This replacement improves the stability of the code by ensuring the interparticle repulsive force (Koshizuka et al., 1998). The Laplacian operator is defined as (Koshizuka et al., 1998):

$$\left\langle \nabla^2 \phi \right\rangle_i = \frac{2D_s}{n_0 \lambda} \sum_{j \neq i} (\phi_j - \phi_i) w\left(\left| \boldsymbol{r}_j - \boldsymbol{r}_i \right| \right) \tag{6}$$

where λ is introduced as:

$$\lambda = \frac{\sum_{j \neq i} w\left(\left| \boldsymbol{r}_j - \boldsymbol{r}_i \right| \right) \left| \boldsymbol{r}_j - \boldsymbol{r}_i \right|^2}{\sum_{j \neq i} w\left(\left| \boldsymbol{r}_j - \boldsymbol{r}_i \right| \right)} \tag{7}$$

The particle number density at particle i and the most commonly applied kernel function in MPS-based calculations are given by Eqs. 8 and 9:

$$\left\langle n \right\rangle_i = \sum_{j \neq i} w\left(\left| \boldsymbol{r}_j - \boldsymbol{r}_i \right| \right) \tag{8}$$

$$w(r) = \begin{cases} \dfrac{r_e}{r} - 1 & 0 \leq r < r_e \\ 0 & r_e \leq r \end{cases} \tag{9}$$

In addition, the pressure is obtained implicitly by solving a Poisson Pressure Equation (PPE):

$$\left(\nabla^2 p_{k+1} \right)_i = \frac{\rho}{(\Delta t)^2} \frac{n_0 - (n_k^*)_i}{n_0} \tag{10}$$

where Δt = calculation time step; and k denotes the step of calculation.

3. MPS METHOD; IMPROVEMENT OF MOMENTUM CONSERVATION

All numerical methods for simulation of hydrodynamic flows are based on the fundamental principles of physics including mass and momentum conservation. Particle methods are not an exception; nevertheless, due to the particle-based discretization, local (and thus global) conservation of momentum may not be ensured in a particle-based calculation unless special attention is focused on the interparticle forces. In a recent study, Khayyer and Gotoh (2008) showed that in standard MPS method, the pressure gradient term does not conserve neither linear nor angular momentum because the interparticle pressure forces are not anti-symmetric (equal in magnitude, opposite in direction). In other words, by considering the original pressure gradient term in MPS method (Eq. 4), the force due to pressure on particle i owing to j would be:

$$\boldsymbol{A}^p_{j \to i} = -m_i \frac{D_s}{\rho n_0} \frac{p_j - \hat{p}_i}{\left| \boldsymbol{r}_j - \boldsymbol{r}_i \right|^2} (\boldsymbol{r}_j - \boldsymbol{r}_i)\, w\left(\left| \boldsymbol{r}_j - \boldsymbol{r}_i \right| \right) \tag{11}$$

while the pressure force on particle j owing to i is:

$$\boldsymbol{A}^p_{i \to j} = -m_j \frac{D_s}{\rho n_0} \frac{p_i - \hat{p}_j}{\left| \boldsymbol{r}_i - \boldsymbol{r}_j \right|^2} (\boldsymbol{r}_i - \boldsymbol{r}_j)\, w\left(\left| \boldsymbol{r}_i - \boldsymbol{r}_j \right| \right) \tag{12}$$

Hence:

$$\boldsymbol{A}^{p}_{j\to i} \neq -\boldsymbol{A}^{p}_{i\to j} \tag{13}$$

Even if p_i had not been replaced with the minimum pressure at neighboring particles as in Eq. 4, the pressure interacting forces would have been equal (if m_i=m_j) in magnitude but not opposite in direction and therefore, not anti-symmetric. For this reason, conservation of both linear and angular momentum is not guaranteed in standard MPS method. However, by deriving an anti-symmetric pressure gradient term, the conservation of both linear and angular momentum would be ensured in a MPS-based calculation. The new anti-symmetric pressure gradient term is derived as (Khayyer and Gotoh, 2008):

$$\langle \nabla p \rangle_i = \frac{D_s}{n_0} \sum_{j \neq i} \frac{(p_i + p_j) - (\hat{p}_i + \hat{p}_j)}{\left| \boldsymbol{r}_j - \boldsymbol{r}_i \right|^2} (\boldsymbol{r}_j - \boldsymbol{r}_i)\, w\left(\left| \boldsymbol{r}_j - \boldsymbol{r}_i \right| \right) \tag{14}$$

The above pressure gradient term preserves both linear and angular momentum, seeing that the pressure interacting forces are both anti-symmetric and radial. The MPS method modified by Eq. 14 is given the name Corrected MPS (CMPS; Khayyer and Gotoh, 2008).

3.1 Refined simulation of a plunging breaker and resultant splash-up

In this section the improved performance of CMPS method is shown by simulating the breaking and post-breaking of a plunging breaker on a constant slope. Breaking and post-breaking of a solitary wave with the incident relative wave height or the ratio of offshore wave height (=H_0) to offshore water depth (=h_0) of H_0/h_0=0.40 is simulated over a slope (=s) of 1:15. The prescribed conditions would lead to a strong plunging breaker in which the plunging jet hits the still water ahead of the wave. Hence, as a result of the momentum exchange between the plunging jet and the wedge-shaped still water, a secondary shoreward directed jet is generated from the impact point. The splash of water in form of a secondary jet, often known as splash-up, is a complex yet important process as it plays an essential role in dissipation of wave energy and momentum transfer.

Since the splash-up is a highly deformed flow characterized by anisotropic strain rates, it would be preferable to obtain the viscous forces from a tensor-type strain-based viscosity term rather than a simplified Laplacian model (Eq. 6). For this reason, we have proposed a tensor-type strain-based viscosity when CMPS method is supposed to calculate a highly anisotropically deformed flow such as the splash-up. The proposed strain-based viscosity term is formulated as (Khayyer and Gotoh, 2008):

$$\left(\nu \nabla^2 \boldsymbol{u} \right)_i = \left(\frac{1}{\rho} \nabla \cdot \boldsymbol{T} \right)_i = \frac{1}{\rho} \sum_{j \neq i}^{N_i} V_j\, \boldsymbol{T}_{ij} \cdot \nabla_i w_{ij} = \frac{1}{\rho n_0} \sum_{j \neq i}^{N_i} \boldsymbol{T}_{ij} \cdot \nabla_i w_{ij} \tag{15}$$

where $\boldsymbol{T}$ = the viscous stress tensor which can be related to the strain rate of flow by the following equation:

$$\boldsymbol{T}_{ij} = 2\mu \boldsymbol{S}_{ij} \quad ; \quad \boldsymbol{S}_{ij} = \begin{bmatrix} \left(\dfrac{\partial u}{\partial x} \right)_{ij} & \left(\dfrac{1}{2} \left[\dfrac{\partial u}{\partial y} + \dfrac{\partial v}{\partial x} \right] \right)_{ij} \\ \left(\dfrac{1}{2} \left[\dfrac{\partial u}{\partial y} + \dfrac{\partial v}{\partial x} \right] \right)_{ij} & \left(\dfrac{\partial v}{\partial y} \right)_{ij} \end{bmatrix} \tag{16}$$

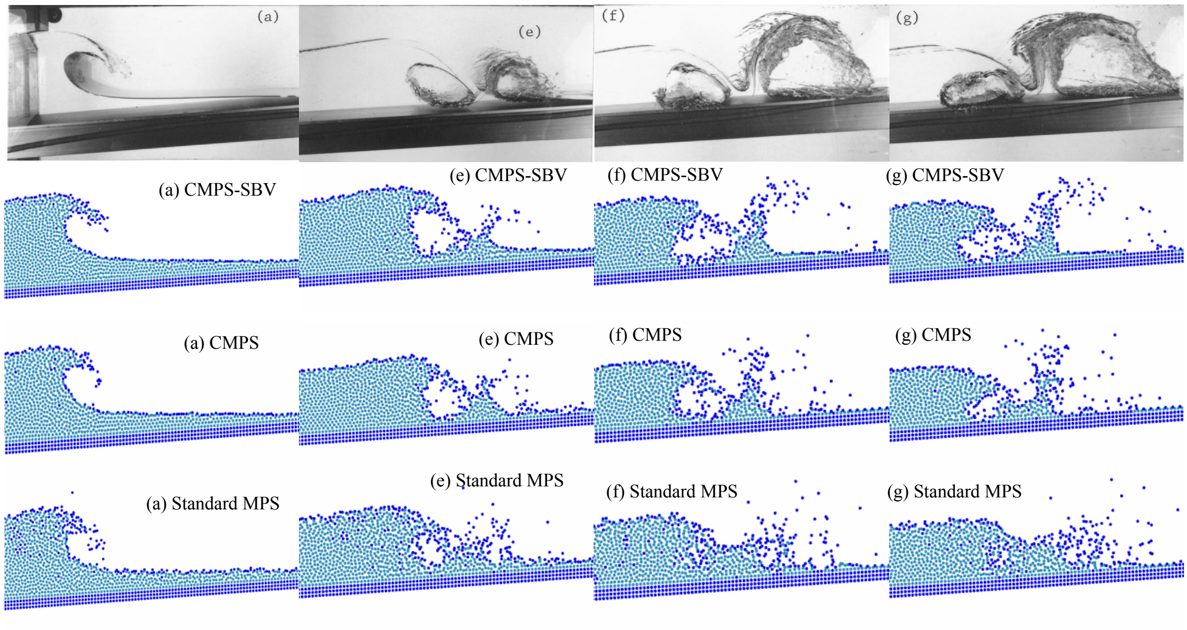

Fig. 1. Refined reproduction of a plunging breaking wave and resultant splash-up - qualitative comparison of laboratory photographs (Li and Raichlen, 2003) with CMPS-SBV, CMPS and standard MPS snapshots

In Eq. 16, μ = dynamic viscosity; u and v = the components of the particle velocity in x and y directions, respectively. The velocity and kernel gradients are introduced for each particle as:

$$\left(\frac{\partial u}{\partial x}\right)_{ij} = \left(\frac{\partial u}{\partial r}\frac{\partial r}{\partial x}\right)_{ij} = \frac{u_{ij}}{r_{ij}}\frac{x_{ij}}{r_{ij}} = \frac{u_j - u_i}{r_{ij}}\frac{x_j - x_i}{r_{ij}} \tag{17}$$

$$\nabla_i w_{ij} = \left(\frac{\partial w_{ij}}{\partial x}\right)_i \boldsymbol{i} + \left(\frac{\partial w_{ij}}{\partial y}\right)_i \boldsymbol{j} = \left(\frac{\partial w_{ij}}{\partial r}\frac{\partial r}{\partial x}\right)_i \boldsymbol{i} + \left(\frac{\partial w_{ij}}{\partial r}\frac{\partial r}{\partial y}\right)_i \boldsymbol{j} = \frac{-r_e x_{ij}}{r_{ij}^3}\boldsymbol{i} + \frac{-r_e y_{ij}}{r_{ij}^3}\boldsymbol{j} \tag{18}$$

The CMPS method with a Strain-Based Viscosity has been given the name CMPS-SBV.

Fig. 1 illustrates the MPS, CMPS and CMPS-SBV snapshots in comparison with their corresponding experimental photographs (Li and Raichlen, 2003). From the figure, the simulation-experiment agreement is better in case of CMPS snapshots compared to those by MPS method. The results by CMPS method portray a clearer image of both plunging jet and the air chamber beneath it with less unphysical particle scattering as seen in MPS snapshots. In addition, from **Fig. 1**(**f**) the splash-up is more precisely simulated by CMPS method rather than by standard MPS method, as the reflected jet angle and the air chamber beneath the plunging jet are in better agreement with the experiment. However, the CMPS method has not been able yet to reproduce the entire curl of the splash-up (**Fig. 1**(**g**)). Further refined reproduction of splash-up is achieved when the viscous interacting forces are obtained by a tensor-type strain-based viscosity in CMPS-SBV method. From **Fig. 1**(**f-g**), the CMPS-SBV method has resulted in an accurate reproduction of splash-up formation and its development with less unphysical particle scattering as seen in CMPS and especially MPS snapshots.

4. MPS METHOD; IMPROVED SOLUTION FOR PRESSURE FIELD

One of the main drawbacks associated with particle methods including the MPS method is the existence of fluctuations in the pressure field. This problem has already been addressed by some researchers including Gotoh et al. (2005) and Colagrossi and Landrini (2003). An improved pressure calculation by a modified Weakly Compressible SPH (WCSPH) method was presented by Colagrossi and Landrini (2003). In their study, density at fluid particles was re-initialized at distinctive time steps through applying a first-order accurate interpolation scheme via the application of a moving-least-square kernel approximation. A more accurate interpolation scheme improves the consistency of mass-area-density and accordingly results in a less-fluctuating and more-accurate source term for pressure equation (equation of state). Hence, a less-fluctuating and more-accurate pressure field would be obtained. In contrast to WCSPH methods, the MPS and Incompressible SPH (ISPH; Shao and Lo, 2003) methods employ a Poisson Pressure Equation (PPE) in which the pressure is a direct function of the time rate of change of particle number density (or density in ISPH method) rather than the density itself. Accordingly, to obtain a less-fluctuating and more-accurate pressure field by MPS method, we propose a more accurate source term of PPE based on a higher order calculation of time rate of change of particle number density.

In standard MPS method an intermediate velocity field $\boldsymbol{u}^*$ is considered as a divergence free velocity field plus the gradient of a scalar field:

$$\boldsymbol{u}_k^* = \boldsymbol{u}_{k+1} + \frac{\Delta t}{\rho}\nabla p \tag{19}$$

The intermediate velocity field is obtained explicitly in the first prediction step, considering the viscosity and gravity terms:

$$\boldsymbol{u}_k^* = \boldsymbol{u}_k + \boldsymbol{g}\Delta t + \nu\nabla^2\boldsymbol{u}_{k\text{-}1}\Delta t \tag{20}$$

In the second correction step a correction for velocity is calculated as:

$$\Delta\boldsymbol{u}_k^{**} = \boldsymbol{u}_{k+1} - \boldsymbol{u}_k^* = -\frac{\Delta t}{\rho}\nabla p \tag{21}$$

The velocities and the number densities in the second process satisfy the mass conservation law as follows:

$$\frac{1}{n_0}\frac{\mathrm{D}n}{\mathrm{D}t} + \nabla\cdot(\Delta\boldsymbol{u}_k^{**}) = 0 \tag{22}$$

In standard MPS method, the assumption is that at each time step the incompressibility is perfectly satisfied, that is to say, the particle number densities are exactly adjusted to n_0. Thus, Eq. 22 is written as:

$$\frac{1}{n_0}\frac{n_0 - n_k^*}{\Delta t} + \nabla\cdot(\Delta\boldsymbol{u}_k^{**}) = 0 \tag{23}$$

From Eqs. 21 and 23, the PPE (Eq. 10) is obtained and solved in the standard MPS method. However, in reality because of the errors generated from the discretization of governing equations and the solution process of the system of linear equations, the particle number density at each time step would not be exactly equal to n_0. As a result, calculation of time variation of n ($\mathrm{D}n/\mathrm{D}t$) is accompanied by numerical errors that are being accumulated as the calculation proceeds. The existence of such accumulative errors would lead to considerable pressure fluctuations and hence, an inaccurate pressure field. Here, we propose another formulation for the calculation of $\mathrm{D}n/\mathrm{D}t$. From Eq. 8:

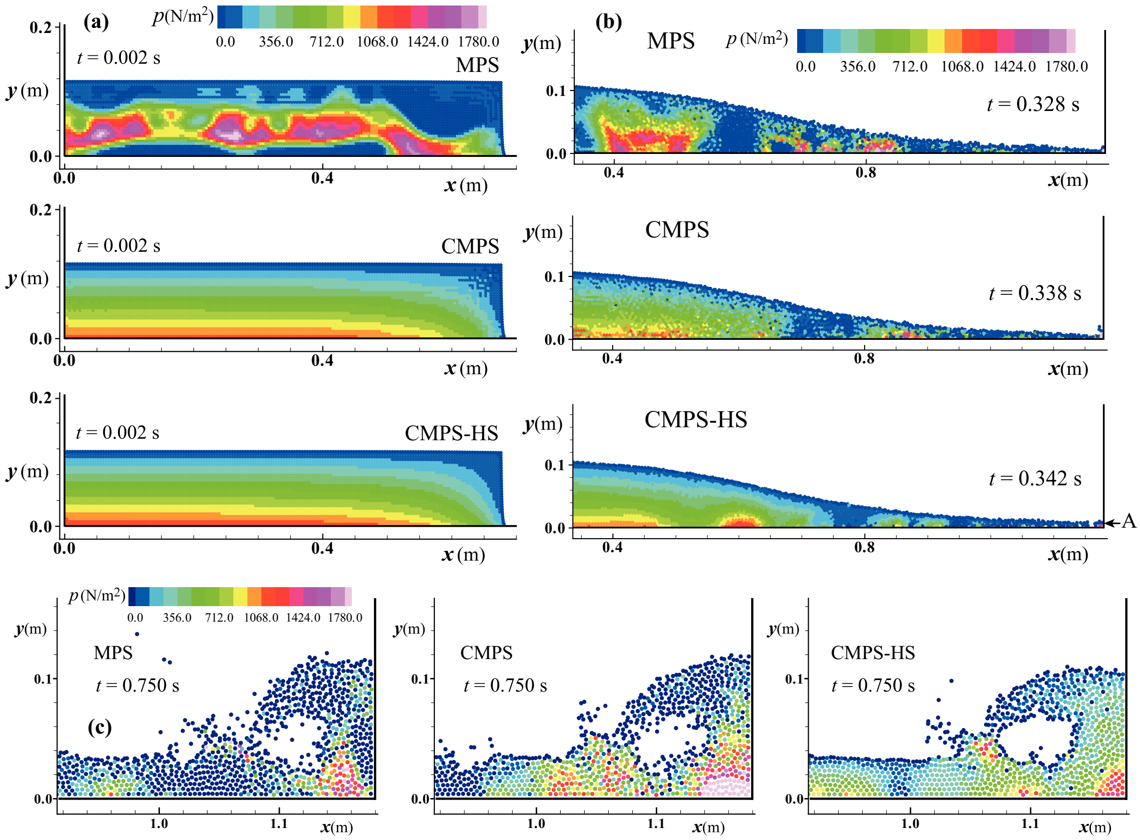

Fig. 2. A dam break with impact - snapshots of water particles together with pressure field

$$\frac{\mathrm{D}n}{\mathrm{D}t}=\sum_{i\neq j}\frac{\mathrm{D}w\left(\left|\boldsymbol{r}_j-\boldsymbol{r}_i\right|\right)}{\mathrm{D}t} \tag{24}$$

By considering the standard kernel in MPS method (Eq. 9):

$$\frac{\mathrm{D}w\left(\left|\boldsymbol{r}_j-\boldsymbol{r}_i\right|\right)}{\mathrm{D}t}=\frac{\mathrm{D}w_{ij}}{\mathrm{D}t}=\left(\frac{\partial w_{ij}}{\partial r_{ij}}\frac{\partial r_{ij}}{\partial x_{ij}}\frac{\mathrm{d}x_{ij}}{\mathrm{d}t}+\frac{\partial w_{ij}}{\partial r_{ij}}\frac{\partial r_{ij}}{\partial y_{ij}}\frac{\mathrm{d}y_{ij}}{\mathrm{d}t}\right)=\left(\frac{-r_e}{r_{ij}^2}\frac{x_{ij}}{r_{ij}}u_{ij}^*+\frac{-r_e}{r_{ij}^2}\frac{y_{ij}}{r_{ij}}v_{ij}^*\right) \tag{25}$$

Therefore, the modified PPE would be:

$$\left(\nabla^2 p_{k+1}\right)_i=-\frac{\rho}{n_0\Delta t}\sum_{i\neq j}\frac{r_e}{r_{ij}^3}\left(x_{ij}u_{ij}^*+y_{ij}v_{ij}^*\right) \tag{26}$$

The CMPS method modified by Eq. 26 is referred as CMPS-HS (CMPS method with a Higher-order Source term). In next two sections, the enhanced performance of CMPS-HS method is shown by simulating a dam break with impact (Hu and Kashiwagi, 2004) and a flip-through impact (Hattori et al., 1994).

4.1 A dam break with impact

In this section, a dam break with impact is simulated by the standard MPS, CMPS and CMPS-HS methods. The physical conditions and the particle size (= 0.004 m) are set equal to those in the study by Hu and Kashiwagi (2004). **Fig. 2**(**a-c**) illustrates the snapshots of water particles together with the pressure field just at the beginning of the dam release (t = 0.002 s); at the time of maximum impact pressure recorded at a point 0.01 m above the bottom (point

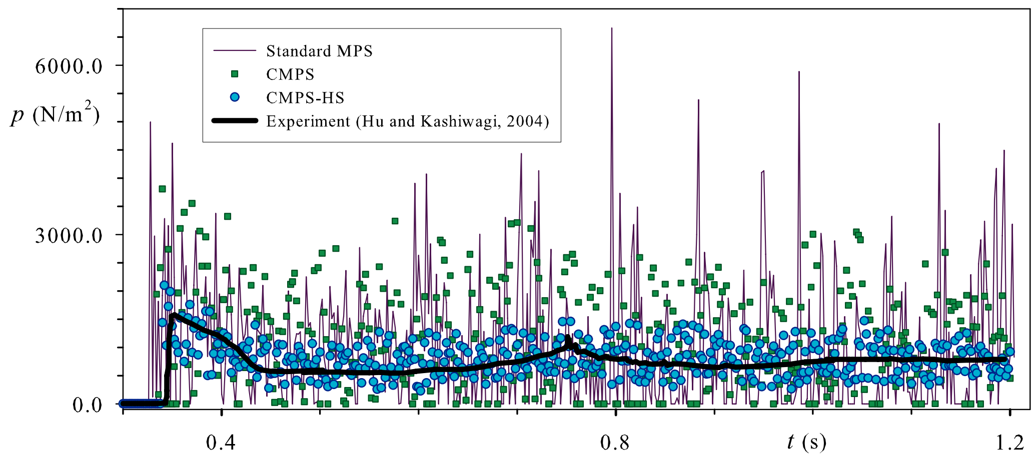

Fig. 3. A dam break with impact - time variation of pressure at measuring point A

A); and at t = 0.750 s which is the experimental time of second peak pressure at point A. From **Fig. 2(a)** it is clear that the standard MPS method has resulted in a false and irregular pressure field even at the beginning of the calculation. The CMPS method has provided a much better pressure distribution. Yet, the curvatures in pressure profile resulting from the difference in accelerations of just-released particles have not been well simulated. Such curved pressure profiles are finely reproduced by CMPS-HS method.

From **Fig. 2(b)**, the pressure distribution by CMPS method appears to be more regular than that by standard MPS method. However, existence of pressure noise is evident in CMPS snapshot. The employment of a higher order source term in CMPS-HS method has removed such pressure noises resulting in a more smoothly-distributed pressure field. After the impact the water is deviated upward and then starts to reverse in form of a plunging jet. Eventually, it impacts the underlying water. **Fig. 2(c)** shows the snapshots of water particles illustrating such violent impact at t = 0.750 s. A spurious pressure distribution together with some unphysical scattering of fluid particles is clear in standard MPS snapshot. The pressure distribution is improved by CMPS method. In addition, the form of the jet appears to be more integrated with less particle scattering. The CMPS-HS method has given a further improved pressure field together with a more integrated plunging jet.

Fig. 3 shows the time variation of pressure at measuring point A. According to the experiment (Hu and Kashiwagi, 2004), the impact pressure (first pressure peak) occurs at $t_{\text{i-exp}}$ = 0.348 s (= experimental impact instant) while the second pressure peak is induced at $t_{\text{sp-exp}}$ = 0.750 s when the plunging jet hits the underlying water and initiates a jet splash-up. Compared to standard MPS and CMPS methods, the CMPS-HS method has resulted in a less-fluctuating and more-accurate pressure calculation. The CMPS-HS has fairly well predicted the values of both first and second pressure peaks, although some amount of overestimation is clear. In addition, the CMPS-HS method has well predicted the impact instant ($t_{\text{i-CMPS-HS}}$ = 0.342 s), the second pressure peak instant ($t_{\text{sp-CMPS-HS}}$ = 0.754 s) and the duration of the first pressure peak. On the other hand, both CMPS and standard MPS methods have underestimated the instants of first pressure peak by 0.010 and 0.020 seconds, respectively. Furthermore, the existence of large-amplitude pressure fluctuations has not allowed both standard MPS and CMPS methods to represent a distinctive second pressure peak.

4.2 A flip-through impact

A flip-through impact without air entrapment is simulated here. The physical and incident wave conditions are set equivalent to those in the experimental study by Hattori et al.

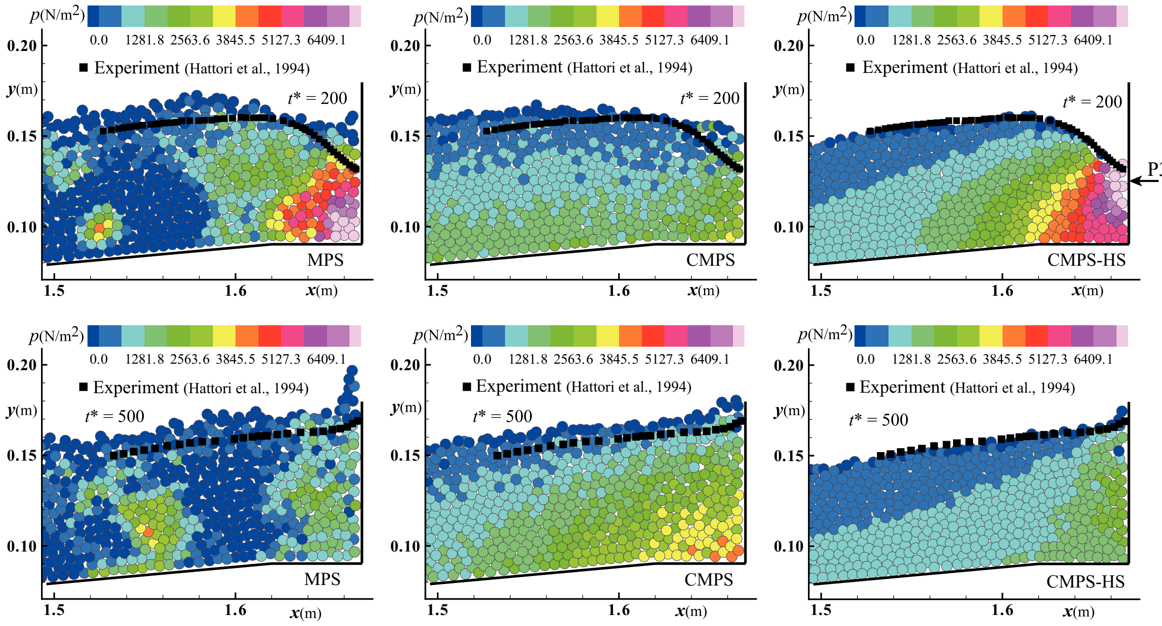

Fig. 4. A flip-through impact - snapshots of water particles together with pressure field at $t^* = 200$ (time of maximum peak pressure recorded at P3) and $t^* = 500$

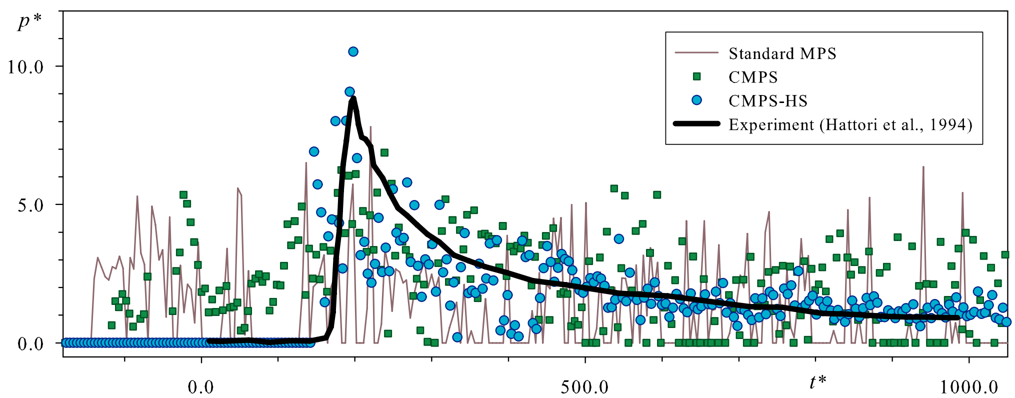

Fig. 5. A flip-through impact - time history of pressure at P3

(1994). **Fig. 4** depicts the snapshots of water particles together with pressure field at $t^* = 200$ and 500. The time of the snapshots are normalized following Hattori et al. (1994): $t^* = t\,C_s/H_F$; C_s = speed of sound = 1500 m/s; H_F = maximum wave height = 0.069 m. In addition, $t^* = 200$ refers to the time of maximum peak pressure recorded at point P3 at the vertical wall at the same elevation of still water level (= 0.125 m). Not surprisingly, the standard MPS method has given a spurious pressure distribution. Both pressure field and free-surface simulation-experiment agreement are improved by CMPS method. A further improved pressure field is obtained by CMPS-HS method. At t^* = 200 the snapshot by CMPS-HS method is characterized by distinctive pressure contours very similar to those calculated by Cooker and Peregrine (1992). From this CMPS-HS snapshot, two other important points can be deduced. Firstly, in agreement with the computation by Cooker and Peregrine (1992), the maximum impact pressure in a flip-through occurs in the vicinity of the still water level. Secondly, the maximum impact pressure at P3 has occurred at an instant very close to that in the experiment since a very good simulation-experiment agreement can be seen in the wave profile. The water surface profile in CMPS-HS snapshot at $t^* = 500$ also closely matches with that from the experiment.

Fig. 5 depicts the time history of pressure at point P3. The vertical and horizontal axes represent the normalized pressure (= $p^* = \rho g/H_F$) and normalized time (= $t^* = t\, C_s/H_F$), respectively. The figure reconfirms the spurious pressure calculation by standard MPS method. The artificial pressure fluctuations seen in standard MPS results are somewhat smoothed in the results by CMPS method. Yet, neither CMPS method nor standard MPS method could provide an acceptable pressure trace. On the other hand, a fairly well agreement can be seen in the results by CMPS-HS method and experimental data.

5. CONCLUSIVE REMARS

Improved MPS methods are proposed for refined simulation of free-surface hydrodynamic flows. By focusing on momentum conservation properties of MPS formulations and pressure solution process, we have proposed two improved MPS methods, namely, Corrected MPS (CMPS; Khayyer and Gotoh, 2008) and CMPS with a Higher-order Source term (CMPS-HS). Enhanced performance of the proposed methods in refined reproduction of both free-surface profile and pressure field is shown through the simulation of numerous hydrodynamic flows with comparison to experiment.

REFERENCES

Colagrossi, A. and Landrini, M. (2003), Numerical simulation of interfacial flows by smoothed particle hydrodynamics, *J. Comput. Phys*., 191, 448-475.

Cooker, M.J., Peregrine, D.H. (1992), Wave impact pressures and its effect upon bodies lying on the sea bed, *Coastal Engineering*, 18 (3-4), 205-229.

Gotoh, H., Ikari, H., Memita, T., Sakai, T. (2005), Lagrangian particle method for simulation of wave overtopping on a vertical seawall, *Coast. Eng. J*., 47(2 & 3), 157-181.

Gotoh, H. and Sakai, T. (1999), Lagrangian simulation of breaking waves using particle method, *Coast. Eng. J.*, 41 (3 & 4), 303-326.

Hattori, M., Arami, A., Yui, T. (1994), Wave impact pressure on vertical walls under breaking waves of various types, *Coastal Engineering*, 22 (1-2), 79–114.

Hu, C.H., Kashiwagi, M. (2004), A CIP Method for Numerical Simulations of Violent Free Surface Flows, *Journal of Marine Science and Technology*, 9 (4), 143-157.

Khayyer, A. and Gotoh, H. (2008), Development of CMPS method for accurate water-surface tracking in breaking waves, *Coast. Eng. J.*, 50(2), 179-207.

Koshizuka, S., Nobe, A., Oka, Y. (1998), Numerical Analysis of Breaking Waves Using the Moving Particle Semi-implicit Method, *Int. J. Numer. Meth. Fluid*, 26, 751-769.

Koshizuka, S. and Oka, Y. (1996), Moving particle semi-implicit method for fragmentation of incompressible fluid, *Nuclear Science and Engineering*, 123, 421-434.

Li, Y. and Raichlen, F. (2003), Energy balance model for breaking solitary wave runup, *Journal of Waterway, Port, Coastal, and Ocean Engineering*, 129(2), 47-59.

Shao, S. D. and Lo, E. Y. M. (2003), Incompressible SPH method for simulating Newtonian and non-Newtonian flows with a free surface, *Advanced Water Resources*, 26 (7), 787-800.